Biochimica et Biophysica Acta 1813 (2011) 1689–1699

Contents lists available at ScienceDirect

Biochimica et Biophysica Acta

journal homepage: www.elsevier.com/locate/bbamcr

Phosphorylation of dynamin II at serine-764 is associated with cytokinesis

Megan Chircop [a,*], Boris Sarcevic [b], Martin R. Larsen [c], Chandra S. Malladi [a], Ngoc Chau [a], Michael Zavortink [a], Charlotte M. Smith [a], Annie Quan [a], Victor Anggono [a], Peter G. Hains [a], Mark E. Graham [a], Phillip J. Robinson [a]

[a] Children's Medical Research Institute, The University of Sydney, 214 Hawkesbury Road, Westmead, NSW 2145, Australia
[b] St. Vincent's Institute of Medical Research and Department of Medicine, St. Vincent's Hospital, The University of Melbourne, Fitzroy, Victoria, Australia
[c] Department of Biochemistry and Molecular Biology, University of Southern Denmark, DK-5230 Odense, Denmark

ARTICLE INFO

Article history:
Received 20 August 2010
Received in revised form 30 November 2010
Accepted 21 December 2010
Available online 29 December 2010

Keywords:
Centrosome
Cytokinesis
Dynamin II
Mitosis
Phosphorylation

ABSTRACT

Calcineurin is a phosphatase that is activated at the last known stage of mitosis, abscission. Among its many substrates, it dephosphorylates dynamin II during cytokinesis at the midbody of dividing cells. However, dynamin II has several cellular roles including clathrin-mediated endocytosis, centrosome cohesion and cytokinesis. It is not known whether dynamin II phosphorylation plays a role in any of these functions nor have the phosphosites involved in cytokinesis been directly identified. We now report that dynamin II from rat lung is phosphorylated to a low stoichiometry on a single major site, Ser-764, in the proline-rich domain. Phosphorylation on Ser-764 also occurred in asynchronously growing HeLa cells and was greatly increased upon mitotic entry. Tryptic phospho-peptides isolated by TiO_2 chromatography revealed only a single phosphosite in mitotic cells. Mitotic phosphorylation was abolished by roscovitine, suggesting the mitotic kinase is cyclin-dependent kinase 1. Cyclin-dependent kinase 1 phosphorylated full length dynamin II and Glutathione-S-Transferase-tagged–dynamin II–proline-rich domain *in vitro*, and mutation of Ser-764 to alanine reduced proline-rich domain phosphorylation by 80%, supporting that there is only a single major phosphosite. Ser-764 phosphorylation did not affect clathrin-mediated endocytosis or bulk endocytosis using penetratin-based phospho-deficient or phospho-mimetic peptides or following siRNA depletion/rescue experiments. Phospho-dynamin II was enriched at the mitotic centrosome, but this targeting was unaffected by the phospho-deficient or phospho-mimetic peptides. In contrast, the phospho-mimetic peptide displaced endogenous dynamin II, but not calcineurin, from the midbody and induced cytokinesis failure. Therefore, phosphorylation of dynamin II primarily occurs on a single site that regulates cytokinesis downstream of calcineurin, rather than regulating endocytosis or centrosome function.

1. Introduction

Dynamin II (dynII) is a large GTPase enzyme that is essential for clathrin-mediated endocytosis (CME). It also plays roles in centrosome cohesion and cytokinesis [1–4]. It is one of three "classical" dynamins (I, II and III) and with a variety of dynamin-related proteins (DRPs) forms the dynamin super family, which is conserved throughout eukaryotes [5]. All members appear to be involved in membrane fission or fusion events. DynI is neuron-specific, dynII is ubiquitously expressed and dynIII has restricted expression primarily in brain and testis [6]. DynII appears to be the ancestral form most closely related to the DRPs found in lower organisms. All dynamin super family proteins contain an N-terminal GTPase domain and a middle domain, while most also have a GTPase effector domain (GED). Interaction between these domains allows for dynamin oligomerisation [7]. The classical dynamins contain two additional domains: a pleckstrin homology (PH) domain for phospholipid binding and a proline-rich domain (PRD) that is the main site of phosphorylation and interacts with SH3 domains from other proteins [8].

DynI and dynIII are phosphorylated in nerve terminals on Ser-774 and Ser-778 (equivalent to Ser-759 and Ser-763 in dynIII) in the phospho-box region of their PRD [9]. DynI is phosphorylated on these sites *in vitro* by the cyclin-dependent kinase (cdk), cdk5 [8] and on Ser-857 by minibrain kinase/Dyrk1A [10]. In addition, we used mass spectrometry to confirm Ser-857 as well as identify Ser-512, Ser-851, Ser-822 and Ser-347 as *in vivo* phosphosites [9]. Whereas dynIII is phosphorylated on only one additional phosphosite, Ser-853, which is equivalent to Ser-851 in dynI [9]. When nerve terminals are depolarised, the resultant Ca^{2+}-influx activates CaN to dephosphorylate dynI [11] and immediately stimulates activity-dependent bulk endocytosis (ADBE) for later formation of new synaptic vesicles by budding from the endosomes [6,12]. These phosphosites regulate protein–protein interactions: Ser-774/Ser-778 dephosphorylation stimulates syndapin recruitment [13,14], whereas Ser-857

* Corresponding author. Tel.: +61 2 9687 2800; fax: +61 2 9687 2120.
E-mail address: mchircop@cmri.org.au (M. Chircop).

0167-4889/$ – see front matter © 2011 Elsevier B.V. All rights reserved.
doi:10.1016/j.bbamcr.2010.12.018

phosphorylation appears to reduce dynI binding to amphiphysin I (amphI) and Grb2, although it is not located within their known binding site [10]. The roles of the other dynI sites or the three phosphosites in dynIII are unknown.

In non-neuronal cells, overexpressed dynI and endogenous dynII are phosphorylated by the tyrosine kinase c-Src at Tyr-231 and Tyr-597 following growth factor stimulation [15,16] and this appears to regulate Golgi integrity and vesicle secretion from the Golgi [17]. Previous systematic phosphosite analysis experiments in nerve terminals revealed no *in vivo* phosphorylation sites identified in rat brain dynII, despite that the protein was readily isolated and detected, indicating that it is not appreciably phosphorylated in nerve terminals despite good protein abundance [9]. Of the seven dynI phosphorylation sites in rat brain, only two are conserved in the dynII amino acid sequence, Ser-347 and Ser-778. This corresponds to rat/human dynII amino acids Ser-347 and Ser-764. Ser-347 phosphorylation accounts for <2% of total dynI phosphorylation and is not dephosphorylated following depolarisation, suggesting it is not a major player in regulating dynI function for ADBE [9]. In contrast, Ser-778 is one of the two major phosphorylation sites that are dephosphorylated following depolarisation. The analogous site, Ser-764, in the dynII phospho-box region is located within a predicted amino acid consensus motif for potential phosphorylation by cdks.

We recently reported that CaN activity is required for cytokinesis and that dynII is one of its substrates at the midbody [18]. DynII is required for the abscission phase of cytokinesis which is delayed or blocked in the presence of small molecular inhibitors and siRNA targeting dynII [4]. A recent manuscript indicated that dynII is phosphorylated by Cdk1/cyclin B1 on Ser-764 and/or Thr-766 during mitosis and that this reduces its ability to bind microtubules [19]. The role of dynII phosphorylation in cytokinesis is unknown. At least three other endocytic proteins are mitotically phosphorylated by cdk, including epsin, eps15 and amphiphysin I [20,21] of which all are CaN targets in nerve terminals [6]. Two large-scale phosphoproteomic screens identified additional endocytic proteins (e.g. synaptojanin, clathrin light chain) that may be mitotically phosphorylated in HeLa cells [22,23]. This raises the question of whether phosphorylation of endocytic proteins during mitosis affects their endocytic and/or mitotic functions. However, shotgun phosphoproteomic screening data require validation of each protein and phosphosite, as the false discovery rate of assigning the correct phosphosite to a peptide is often unacceptably high. Therefore, our first aim was to use several approaches to directly identify the *in vivo* dynII serine/threonine phosphorylation sites and to confirm which are genuine *in vivo* mitotic phosphosites. We found that it is mitotically phosphorylated by cdk1 in HeLa cells at a single detectable site in the phospho-box, Ser-764. We then aimed to reveal the role of dynII–Ser-764 phosphorylation during mitosis since the analogous site in dynI controls endocytosis. Surprisingly, phosphorylation was not involved in CME or centrosome localisation but specifically targets dynII to the midbody and is involved in cytokinesis.

2. Materials and methods

2.1. siRNA and plasmid construction

Stealth siRNAs targeting human dynamin (dyn, 5′-UCUCCUGCCG-GACUUCAUCAAAGUC-3′) and luciferase (luc, 5′-CGUACGCGGAAUA-CUUCGATT-3′) were purchased from Invitrogen. GFP-α-tubulin was obtained from Jenny Stow (Institute for Molecular Biosciences, Australia). A rat dynamin II cDNA encoding the “aa” splice variant was isolated from a brain cDNA library (Invitrogen) and cloned into pEGFP-C1 as an Eco*R*I and Bam*H*I fragment to generate GFP–dynIIwt. The proline-rich domain (PRD) of rat dynII was amplified using GFP-dynIIwt as a template, then cloned into pGEX-1λT as a Bam*H*I fragment to generate wild-type GST–dynII–PRD (amino acids 740–870). Phospho-deficient (Ser-764A and Ser-764A/T766A) and phospho-mimetic (Ser-764E and Ser-764E/T766E) mutant forms of GFP–dynII (full length and PRD) and a phospho-deficient (Ser-764A) form of GST–dynII–PRD were generated using the QuickChange site-directed mutagenesis kit (Stratagene). The identity of plasmid constructs were confirmed by sequencing and details of primers are available upon request. GST–human amphiphysin II (amphII)–SH3 domain (residues 499–593), in a pGEX-2T plasmid as described [24], GST–rat dynII–PRDwt (amino acids 740–870) and GST–dynII–PRD–Ser-764A fusion proteins were expressed in *Escherichia coli* and purified using glutathione-sepharose beads (Amersham Biosciences) according to the manufacturer's instructions.

2.2. Cell culture and transfection

HeLa cells were maintained in RPMI 1640 medium supplemented with 10% foetal bovine serum (FBS) and grown at 37 °C in a humidified 5% CO_2 atmosphere. Cells were seeded at 50%–60% confluence and transfected with the 1.5 μg of the indicated GFP-tagged plasmid/well of a 6-well plate using Lipofectamine 2000 (Invitrogen) according to the manufacturer's instructions. For siRNA analysis, HeLa cells were transfected with 1000 pmol of siRNA (per 10 cm^2 dish) using Lipofectamine 2000 (Invitrogen). Cells were collected five days post-transfection for immunoblotting. For siRNA rescue assays, cells (2.5×10^5) were co-transfected with 200 pmol of siRNA (against human dynII) and 1.2–1.4 μg of the indicated plasmid DNA (from rat dynII) using 4 μl of Lipofectamine 2000 (Invitrogen) following the manufacturer's general protocol. This rat dynII sequence varies in 6 positions from the human siRNA target region sequence, making it immune from the siRNA treatment. Cells were trypsinized and re-seeded at 48 h after transfection then assayed for transferrin (Tfn) uptake the following day.

2.3. Cell synchronisation and treatments

Cells grown on coverslips were synchronised at the G_1/S border by double thymidine block. Cells were then released into the cell cycle following thymidine wash-out as previously described [25]. At 8 h post-release cells were treated with 100 μM of the dynII peptide for 10 h then fixed for immunofluorescence microscopy analysis. For mitotic synchronization, cells were treated with 0.5 μg/ml nocodazole for 16 h. Mitotic arrested cells were collected by “mitotic shake-off” for immunoblot analysis. For cdk inhibition, cells were treated with 10 μM roscovitine either alone or in combination with nocodazole. Under these conditions only mitotically rounded cells were collected and analysed. Alternatively, cells were synchronised at the G_2/M border by treatment with the selective cdk1 small-molecule inhibitor, RO-3306 (9 μM) for at least 18 h [26]. Cells were allowed to progress through mitosis following RO-3306 wash-out. Where indicated, cells were treated with 100 μM of the dynII peptide immediately following RO-3306 wash-out and incubated at 37 °C/5% CO_2 for 1.5 h (metaphase localization analysis), 3 h (cytokinesis localization analysis) or 6 h (multinucleation scoring).

2.4. Antibodies

The following antibodies were used: anti-dynII (C-18, Santa Cruz Biotechnology), anti-dynI, anti-dynI phospho-Ser-774 and anti-dynI phospho-Ser-778 [13], anti-cyclin B1 (V152; Cell Signaling), anti-α-tubulin (clone DM1A; Sigma) and anti-γ-tubulin (GTU88; Sigma).

2.5. Immunoblotting

Cellular extracts were prepared by incubating HeLa cells in ice-cold lysis buffer (25 mM Tris–HCl pH 7.4, 150 mM NaCl, 1 mM EDTA, 1 mM EGTA, 1 mM PMSF, 1% Triton X-100, and EDTA-free Complete

protease inhibitor cocktail (Roche)) and the supernatant was collected following centrifugation at 13,000 rpm for 30 min at 4 °C. DynII protein was enriched by incubating the cellular extracts with purified GST–amphII–SH3 domain bound to glutathione-sepharose beads for 1 h at 4 °C. Beads were washed extensively with ice-cold lysis buffer. Bound proteins were fractionated by SDS–PAGE for immunoblot analysis. Primary antibody was applied then detected by with a horseradish peroxidase-conjugated secondary antibody (Sigma). Blotted proteins were visualised using the ECL detection system (Pierce).

2.6. Antarctic phosphatase treatment

For dephosphorylation, mitotic HeLa cell lysates were prepared and the sample was enriched for dynII protein by performing a pull-down with 100 µl of a 50% slurry of GST–amphII–SH3 as described above. Beads were washed twice with ice-cold wash buffer (20 mM ammonium bicarbonate, pH 8.0), then resuspended in ice-cold reaction buffer (20 mM ammonium bicarbonate, 1 mM $MgCl_2$, pH 8.0). Antarctic phosphatase (AP, 5 µl, New England Biolabs) was added and the reaction was incubated for 2 h at 15 °C before the beads were washed to remove the phosphatase.

2.7. In vitro protein phosphorylation

DynI was purified by a GST–amphII–SH3 pull-down from total sheep brain extract, as described previously for rat brain [13]. DynII (100 µg) was purified from baculovirus-infected Sf9 insect cells (provided by SL Schmid, the Scripps Research Institute, CA) but had a high level of endogenous phosphorylation that required prior removal. DynI and dynII were diluted in Tris buffer (20 mM Tris–HCl pH 7.4, 1 mM DTT, 150 mM NaCl and EDTA-free Complete protease inhibitor cocktail), bound to GST–amphII–SH3 beads, washed twice and incubated overnight with AP at 4 °C and dephosphorylated dynI and dynII were eluted twice with Tris–HCl buffer containing 1.2 M NaCl. The eluted fractions were pooled and microdialysed (Pierce) against Tris buffer containing 20% glycerol and 100 mM NaCl. Dephosphorylated native dynI and dephosphorylated baculovirus expressed dynII were then used as *in vitro* substrates for purified recombinant cdk1/cyclin B1, cdk1/cyclin A, cdk2/cyclin A, cdk2/cyclin E, cdk4/cyclin D1 and MAPK kinase as described previously [27]. Where indicated, purified recombinant pRb and dynII purified from rat liver were used as substrates. Alternatively, purified bacterially expressed wild-type and phospho-deficient (Ser-764A) forms of GST–dynII–PRD were used as substrates for cdk1/cyclin A.

2.8. Nano-liquid chromatography mass spectrometry (nanoLC–MSMS)

Lungs were excised from two rats or 10^7 mitotic synchronised HeLa cells were used to make lysates from which dynII protein was enriched by performing a GST–amphII–SH3 pull-down as described above. Proteins were resolved by SDS–PAGE and visualised on the gel by staining with colloidal Coomassie blue. DynII SDS–PAGE gel bands, estimated at 1–5 pmol protein from human mitotic cells or 10–20 pmol from rat lung, were digested with trypsin and phosphopeptides were enriched using titanium dioxide as described previously [28]. The rat lung dynII tryptic digest was further digested with Asp-N because the tryptic phospho-box peptide was considered too long for correct assignment of the phosphorylation site. An aliquot of the phospho-peptide-enriched human or rat dynII digest was injected into a nano-HPLC system (LC Packings Ultimate HPLC system, Dionex, Netherlands) and the eluate was analysed by a QSTAR XL quadrupole-TOF MS (Applied Biosystems, USA) or QTOF Premier (Waters, UK) as described previously [29]. Spectra were recorded using information-dependent data acquisition. Phosphopetide tandem mass spectra were exported to Mascot 2.2 (Matrix Science, UK) for automated database searching and identification. They were also manually examined to determine the phosphorylation sites.

2.9. Immunofluorescence microscopy

Cells were fixed in ice-cold 100% methanol for 10 min at −20 °C and then blocked in 3% bovine serum albumin/PBS for 45 min before the required primary antibody was applied. Cells that were transfected with GFP–dynII–PRD plasmids were fixed in 4% paraformaldehdye/PBS. Fluorescein- or Texas Red dye-conjugated AffiniPure secondary antibodies (Jackson ImmunoResearch Laboratories, Inc.) were then applied. Cell nuclei were counterstained with DAPI (4′, 6′-diamidino-2-phenylindole; Sigma). Cells were washed three times with PBS between each step except after blocking. Cells were viewed and scored with a fluorescence microscope (Ziess). Fluorescence images were captured under an Olympus IX80 inverted microscope using 100× oil immersion lenses and deconvolved using AutoDeblur v9.3 (AutoQuant Imaging, Watervliet, NY).

2.10. Endocytosis assay

Quantitative high-throughput receptor-mediated endocytosis (RME) assays were performed by an automated process as previously described [30,31] using Texas Red-Transferrin (Tfn), Texas Red-epidermal growth factor (EGF), and FITC-dextran uptake in cultured U2OS and HeLa cells pretreated with penetratin-coupled dynII peptides for 30 min. IC_{50} values were calculated using Prism 5 (GraphPad Software Inc.) and data are expressed as mean ± 95% confidence intervals (CI) for triplicates and ~1200 cells.

3. Results

3.1. DynII phosphorylation at Ser-764 by cdk1/cyclin B1

Of the two main dynI phosphosites (Ser-774 and Ser-778), only Ser-778 is conserved in the dynII phospho-box at position Ser-764 (Fig. 1A), but this site is not detectably phosphorylated in dynII from nerve terminals [9]. Ser-764 precedes a proline residue. Therefore, we used *in vitro* protein kinase phosphorylation assays to ask whether a cdk could phosphorylate dynII–Ser–764. DynII was phosphorylated *in vitro* by cdk1/cyclin A, cdk1/cyclin B1, cdk2/cyclin A and cdk2/cyclin E complexes with similar efficiency using [γ-^{32}P]ATP labelling (Fig. 1B and D). This phosphorylation was specific, as Cdk4/cyclin D1 did not phosphorylate dynII yet was fully active on a reference substrate—Rb protein (Fig. 1D). Another proline-directed kinase, mitogen-activated protein kinase (MAPK), also phosphorylated both dynamin proteins to a lesser extent (Fig. 1B and C). To determine if dynII–Ser-764 was a site of phosphorylation we used a phospho-specific antibody. The phospho-peptide amino acid sequence used to generate the dynI phospho-Ser-778 antibody is conserved in dynII (underlined in Fig. 1A) except for the single N-terminal residue. We have previously shown that this antibody recognises dynII phosphorylated at Ser-764 [18]. This antibody recognised cdk1-mediated phosphorylated dynII *in vitro*, indicating that cdk targets Ser-764 (Fig. 1B). As a control, dynI was phosphorylated on Ser-778 *in vitro* by both cdk1/cyclin A and cdk1/cyclin B1 as indicated by both [γ-^{32}P]ATP labelling and Western blot analysis with the phosphosite-specific antibody (Fig. 1C), consistent with previous reports [8]. Phosphorylation detected by both [γ-^{32}P]-ATP labelling and the phosphosite-specific antibody matched for each protein kinase, suggesting dynII is phosphorylated on the analogous site, Ser-764 in the PRD. This was confirmed by MS analysis (see below).

We next aimed to determine whether other phosphosites were targeted by cdk1 in the dynII PRD. As found for full length dynII (Fig. 1B), GST–dynII–PRDwt protein was efficiently phosphorylated

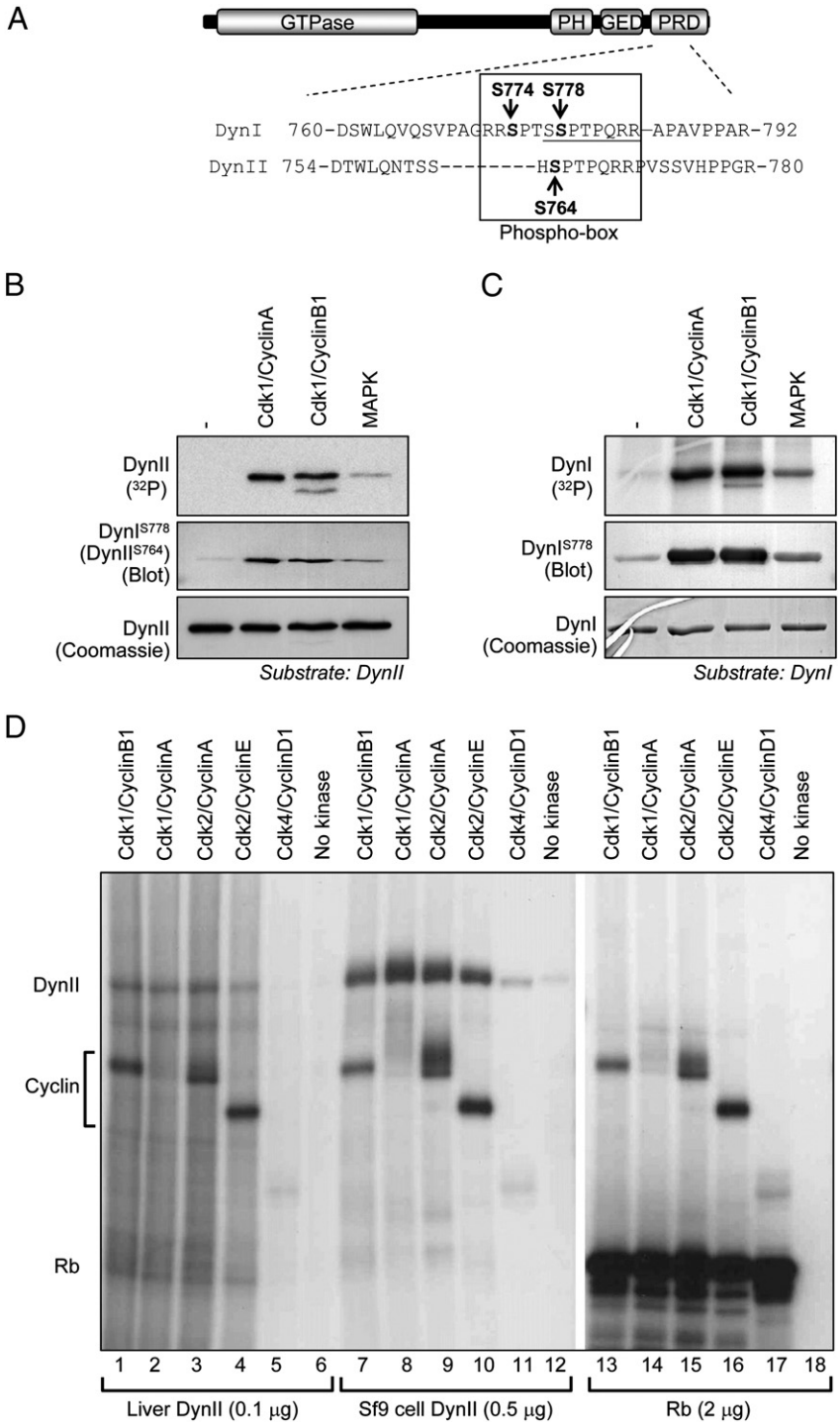

Fig. 1. DynII is phosphorylated by the mitotically active kinase, cdk1/cyclin B1 on Ser-764. (A) Dynamin consists of four major domains: the GTP hydrolysis domain (GTPase), a pleckstrin homology (PH) domain, a GTPase effector domain (GED) and a proline-rich domain (PRD). DynI is phosphorylated by cdk5 at Ser-774 and Ser-778 (bold amino acids) *in vivo* in the 'phospho-box' region. Of these two phosphorylation sites, only Ser-778 is conserved in dynII as an SP motif, corresponding to residue Ser-764 (bold). The amino acid sequence underlined in dynI was the peptide used to generate the phospho-Ser-778 specific antibody [13]. (B and C) *In vitro* protein kinase assay. Purified cdk1/cyclin A, cdk1/cyclin B1 and MAPK were examined for their ability to phosphorylate purified dynII and dynI at Ser-764 and Ser-778, respectively, in an *in vitro* protein kinase assay. DynII (B) and dynI (C) phosphorylation were determined by [γ-^{32}P]-ATP labelling (upper panel) and Western blotting (middle panel) with the phospho-specific antibody anti-dynI–Ser-778. (D) *In vitro* phosphorylation of dynII by Cdk/cyclin complexes. Purified cdk1/cyclin A, cdk1/cyclin B1, cdk2/cyclin A, cdk2/cyclin E and cdk4/cyclin D1 kinases were examined for their ability to phosphorylate dynII, which had been purified from rat liver (0.1 μg, lanes 1–6) and from baculovirus (0.5 μg, Sf9 cells; lanes 7–12) in an *in vitro* protein kinase assay. Rb (2 μg) was phosphorylated with the same kinases (lanes 13–18) and served as a positive control. Phosphorylation was determined by [γ-^{32}P]ATP labelling. DynII was phosphorylated by all cdk/cyclin protein kinase complexes except for cdk4/cyclin D1. Blots shown in (B–D) are representative of at least two independent experiments.

by cdk1 *in vitro* using [γ-^{32}P]-ATP labelling and phosphorylation increased in a time-dependent manner (Fig. 2). Phosphorylation was greatly reduced when Ser-764 was mutated to alanine (Fig. 2). Less than 20% of the total phosphorylation remained in this mutant, suggesting that Ser-764 is the major *in vitro* phosphorylation site by cdk1 within the dynII–PRD.

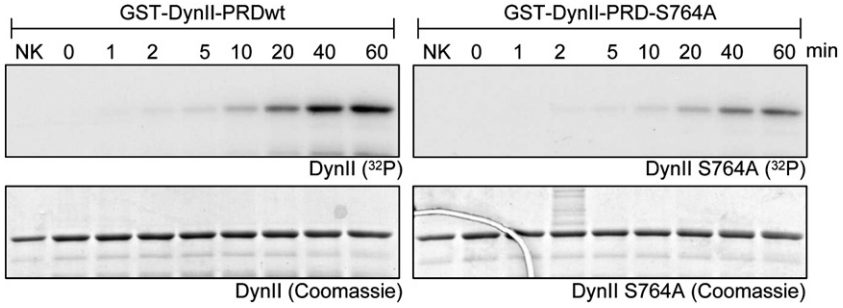

Fig. 2. Mutation of Ser-764 reduces cdk1-mediated phosphorylation of dynII *in vitro*. GST–dynII–PRD wt was phosphorylated by cdk1/cyclin A as determined by [γ-^{32}P]-ATP labelling and this increased with time. Cdk1/cyclin A-mediated phosphorylation was significantly reduced by mutation of Ser-764 to alanine. NK, no kinase. The upper panels are autoradiographs (^{32}P) of phosphorylated GST–dynII–PRDwt (left) or GST–dynII–PRD—S764A (right), with the corresponding Coomassie stained gels in the panels below (Coomassie). Blots are representative of two independent experiments.

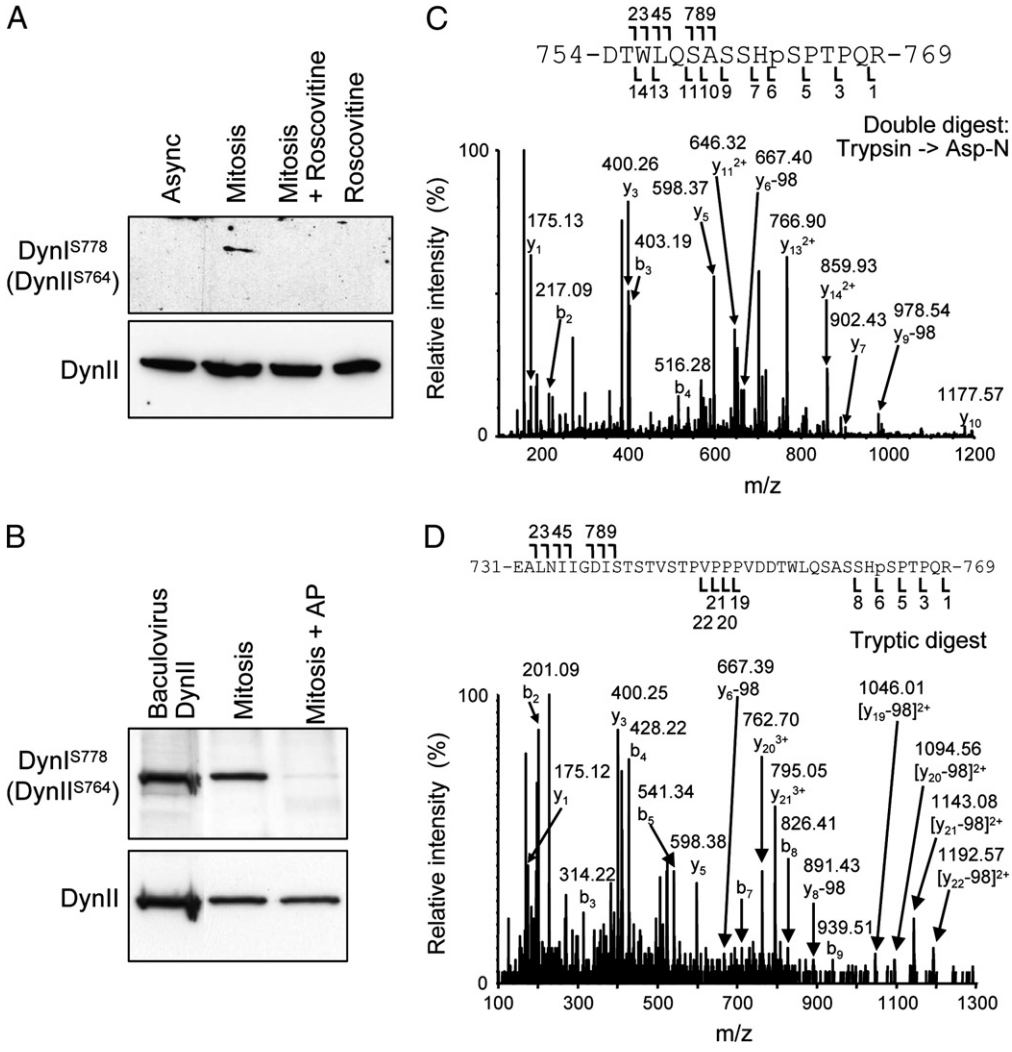

Fig. 3. DynII is phosphorylated at Ser-764 during mitosis. (A) Asynchronous and mitotically synchronised HeLa cells were treated with the cdk inhibitor, roscovitine (10 μM) for 16 h. Whole cell lysates (100 μg) were blotted for the phosphorylation status of dynII at Ser-764 and for dynII levels. (B) Lysates from HeLa cells synchronised in prometaphase were treated with or without Antarctic phosphatase (AP). DynII purified from baculovirus-infected Sf9 cells served as a control. Samples were blotted for the phosphorylation status of dynII and for dynII levels. Blots shown in panels A and B are representative of three independent experiments. (C) Native dynII was purified from rat lung and doubly digested with trypsin followed by Asp-N. Analysis of the titanium dioxide enriched fraction of this digest revealed a single phospho-peptide that was sequenced by tandem mass spectrometry. Fragmentation of the triply charged precursor at m/z 626.6 produced a spectrum matching the sequence of rat dynII$_{754–769}$ where Ser-764 is phosphorylated (shown as pS). The phosphorylation site was readily revealed as the molecular mass of a dehydroalanine residue (69 Da) between y_5 and y_6-98 ions resulting from the neutral loss of phosphoric acid (−98 Da) from the phosphoserine residue. (D) Phosphorylated dynII was isolated from mitotically synchronised HeLa cells. A single phosphorylated tryptic peptide was found and its phosphorylation site was sequenced by tandem mass spectrometry. Fragmentation of the quadrupally charged precursor at m/z 1046.3 produced a spectrum matching the sequence of human dynII$_{731–769}$ where Ser-764 is phosphorylated. Although this peptide was longer than the rat dynII peptide, the fragmentation information from the C-terminal end was the same. The phosphorylation site was unequivocally revealed between the y_5 and y_6-98 ions.

3.2. DynII is mitotically phosphorylated at Ser-764 by cdk1

Several components of the endocytic machinery are mitotically phosphorylated—epsin, eps15 [20], amphiphysin [21] and Drp1 [32]. Since dynII is phosphorylated by the mitotic kinase, cdk1/cyclin B1, and dephosphorylated by CaN during cytokinesis [18], we asked whether phosphorylation is increased during mitosis in HeLa cells. DynII phosphorylation at Ser-764 was barely detectable in asynchronously growing cells but was markedly increased in mitotically synchronised cells (Fig. 3A). This was prevented by treatment with the cdk inhibitor, roscovitine (Fig. 3A), suggesting that cdk1 is the responsible *in vivo* protein kinase. The dynI phospho-Ser-774 antibody did not recognise any HeLa cell proteins in the 90–110 kDa region, consistent with undetectable expression of dynI in these cells (data not shown) and lack of conservation of Ser-774 in the dynII sequence (Fig. 1A). Antarctic phosphatase treatment of lysates from mitotically synchronised HeLa cells abolished phospho-Ser-778 antibody labelling (Fig. 3B), confirming that the band detected during mitosis represented *bona fide* dynII phosphorylation. Thus, Ser-764 on dynII is mitotically phosphorylated.

3.3. Identification of Ser-764 phosphorylation by mass spectrometry

We used comprehensive mass spectrometry analysis of dynII to determine the number and site(s) of phosphorylation on dynII. Tandem mass spectrometry on a QTOF Premier (Waters, UK) revealed that native dynII purified from two rat lungs was phosphorylated on a single site *in vivo* at Ser-764 (Fig. 3C). This identification required a large amount of tissue and extracted dynII to be detectable, thus, is likely to be very low stoichiometry. To directly identify the mitotic phosphorylation site in human dynII, the protein was enriched from mitotically synchronised HeLa cells by binding to GST–amphII–SH3 attached to GSH sepharose, which quantitatively binds all three classical dynamins [9]. Tryptic digests analysed by tandem mass spectrometry exclusively detected dynII, confirming the lack of detectable expression of dynI or III in these cells. In at least six independent experiments, a single phospho-peptide was found and the site was assigned to Ser-764 in dynII (Fig. 3D). At no point were other phospho-peptides or phosphosites identified.

3.4. Phosphorylation at Ser-764 is not required for clathrin-mediated and bulk endocytosis

To gain insight into the biological significance of dynII–Ser-764 phosphorylation, we sought to determine its effect on endocytosis by using a penetratin-based membrane permeable peptide strategy [12,13,33]. Phospho-mimetic peptides were designed to mimic the amino acid sequence of the dynII phospho-box and were tagged with a short penetratin heptapeptide to facilitate their delivery into cells (Fig. 4A). This strategy prevents indirect or long-term effects caused by overexpressing dynII phosphosite mutants and avoids variability in transfection efficiency. It has been validated in several previous studies, such as in determining the role of dynI dephosphorylation in

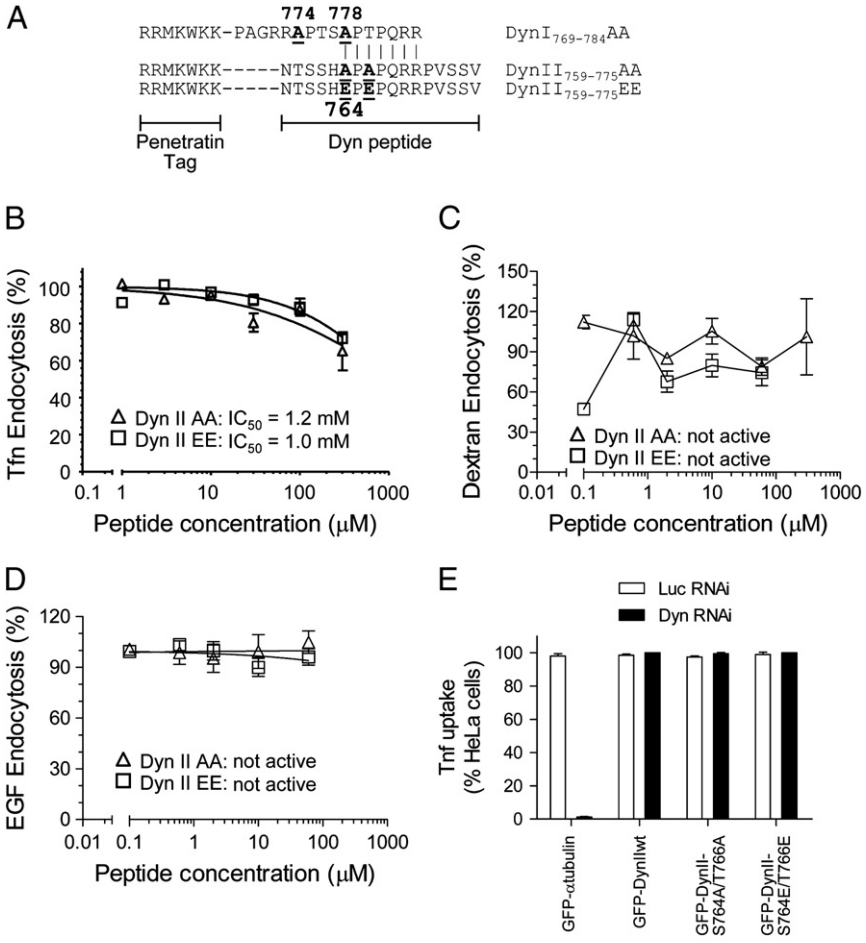

Fig. 4. Ser-764 phosphorylation is not required for endocytosis. (A) Sequences of penetratin-linked peptides synthesised from the phospho-box region. (B–D) Quantitative high-throughput endocytosis assays were performed by an automated process using Texas Red-Tfn (B), Texas Red-EGF (C) and FITC-dextran (D) uptake in cultured U2OS cells pretreated with the dynII peptides for 30 min. Data are expressed as mean ± 95% confidence intervals (CI) for triplicates and ~1200 cells. Similar results were obtained in three independent experiments. (E) Quantitation of the percentage of HeLa cells that have endocytosed Texas Red-Tfn following co-transfection with the indicated siRNA and either GFP-tubulin or the indicated rat GFP–dynII plasmid. DynII–Ser-764 phospho-deficient and phospho-mimetic mutants rescue endocytosis of Tfn as efficiently as wild-type GFP–dynII.

stimulating recruitment of the dynI partner syndapin I [12,13]. In those studies, the homologous phospho-box AA peptide designed against the sequence of dynI (Fig. 4A) potently inhibits ADBE by preventing the dynI/syndapin I interaction, while it is without effect on transferrin endocytosis in U2OS cells which lack dynI. Thus, it was possible that the analogous dynII peptide would inhibit CME. However, neither the dynII$_{759–775}$EE phospho-mimetic peptide nor the dynII$_{759–775}$AA phospho-deficient peptide had significant effects on endocytosis of transferrin (Fig. 4B) or EGF (Fig. 4C) in U2OS cells. Only at extremely high concentrations was endocytosis of transferrin slightly inhibited; however, this was not significant. Endocytosis of dextran, the fluid phase-marker of bulk endocytosis, was also not affected by either dynII phospho-peptide (Fig. 4D). Similar findings were observed in HeLa cells (Supplementary Fig. 1). This suggests that Ser-764 phosphorylation does not regulate the endocytic function of dynII.

To independently ask whether there is a role for Ser-764 in endocytosis, we performed a rescue experiment following depletion of dynII by siRNA. An siRNA sequence common to human dynI, II and III resulted in >90% depletion of dynII and a block in endocytosis of transferrin (data not shown and Fig. 4E). We aimed to rescue this phenotype by overexpressing rat GFP–dynII since the rat sequence varies in 6 positions from the human siRNA target region sequence and is resistant to the siRNA treatment. Ectopic expression of wild-type rat GFP–dynII completely restored endocytosis (Fig. 4E). In contrast, endocytosis was not restored in cells expressing GFP-α-tubulin. Consistent with the results obtained with the phospho-peptide strategy, endocytosis was completely restored in cells ectopically expressing either the phospho-deficient (Ser-764A/Thr-766A) or phospho-mimetic (Ser-764E/Thr-766E) forms of GFP–dynII (Fig. 4E). This indicates that Ser-764 phosphorylation is not required for the endocytic function of dynII. Thus, dynII–Ser-764 phosphorylation may be specifically involved in a mitosis-specific role that is independent of endocytosis.

3.5. DynII localisation to the mitotic centrosome is not dependent on Ser-764 phosphorylation

DynII has been implicated in centrosome cohesion [3] and cytokinesis [1,2,4,34,35]. The centrosome is a critical component for mitosis as it forms the poles of the mitotic spindle. DynII localises to the interphase centrosome and participates in centrosome cohesion [3]. We now show by immunostaining with the dynII–Ser-764 phospho-specific antibody that dynII locates to the mitotic centrosome and is primarily in the phosphorylated form (Fig. 5A). As cells progress through mitosis (metaphase to anaphase/telophase) phospho-dynII remains associated with the centrosome until a late stage, cytokinesis (see below). Centrosomal localisation of phospho-dynII was not disrupted by the dynII$_{759–775}$EE or dynII$_{759–775}$AA peptides (Fig. 5B). Therefore Ser-764 phosphorylation appears not to target or tether dynII to the mitotic centrosome. Unfortunately, attempts to address this question by transfection with GFP-tagged dynII were unsuccessful since, in contrast to native dynII, none of our ectopically expressed proteins (wt, S764A or S764E; C-terminal GFP-tagged dynII, N- or C-terminal FLAG-tagged dynII) were associated with the centrosome possibly due to different expression levels, processing or subcellular distribution. Despite this, a GFP-tagged middle domain of dynII did localise at the centrosome as previously observed [3], supporting our findings that the PRD is not required for centrosome tethering. Thus, full length GFP-dynII does not always mimic the behaviour of endogenous dynamin in all roles.

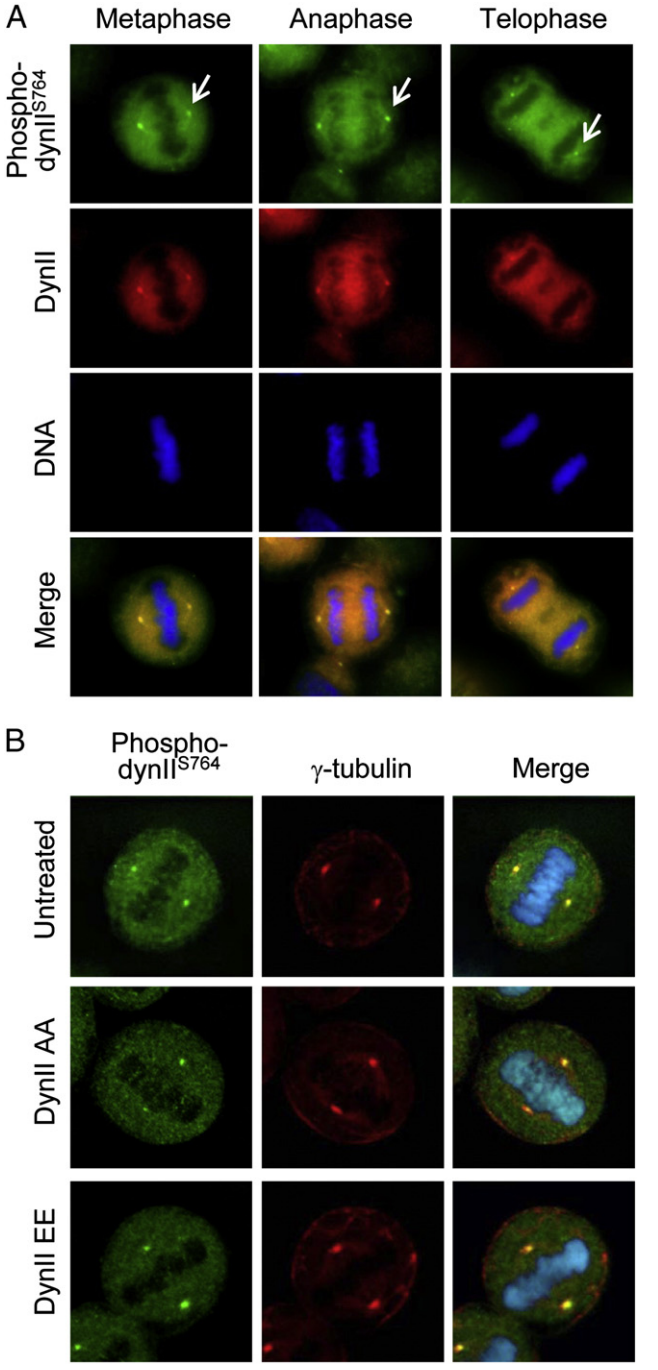

Fig. 5. Ser-764 phosphorylation is not required for targeting dynII to the mitotic centrosome. (A) Phospho-dynII localises to the mitotic centrosome. Asynchronously growing HeLa cells were stained for endogenous phospho-dynII–Ser-764 (green) and total dynII protein (red). Representative cells from different stages of mitosis are shown, illustrating phosphorylated dynII initially at the mitotic centrosome and later at the midbody during cytokinesis. The position of phospho-dynII is shown with arrows (all panels). (B) Representative microscopy images of HeLa cells in metaphase treated in the absence and presence of the DynII-AA and DynII-EE peptide. Phospho-dynII–Ser-764 mitotic centrosome localisation is not disrupted by treatment with either peptide. γ-tubulin (red) served as an independent centrosome marker.

3.6. Ser-764 phosphorylation is associated with dynII midbody localisation and cytokinesis

CaN and phospho-dynII localise to the midbody during cytokinesis [18] and both are required for the abscission stage of cytokinesis [1,2,4]. The phosphatase activity of CaN is specifically associated with completion of cytokinesis and dynII is one of its substrates [18]. Thus, we next asked whether this involves dynII–Ser–764 phosphorylation since phospho-dynII is enriched at the midbody 2.5 h after the onset of mitosis [18]. We now show that midbody localisation was unaffected by treatment with the phospho-deficient peptide (Fig. 6A). In contrast, phospho-dynII was undetectable at the midbody

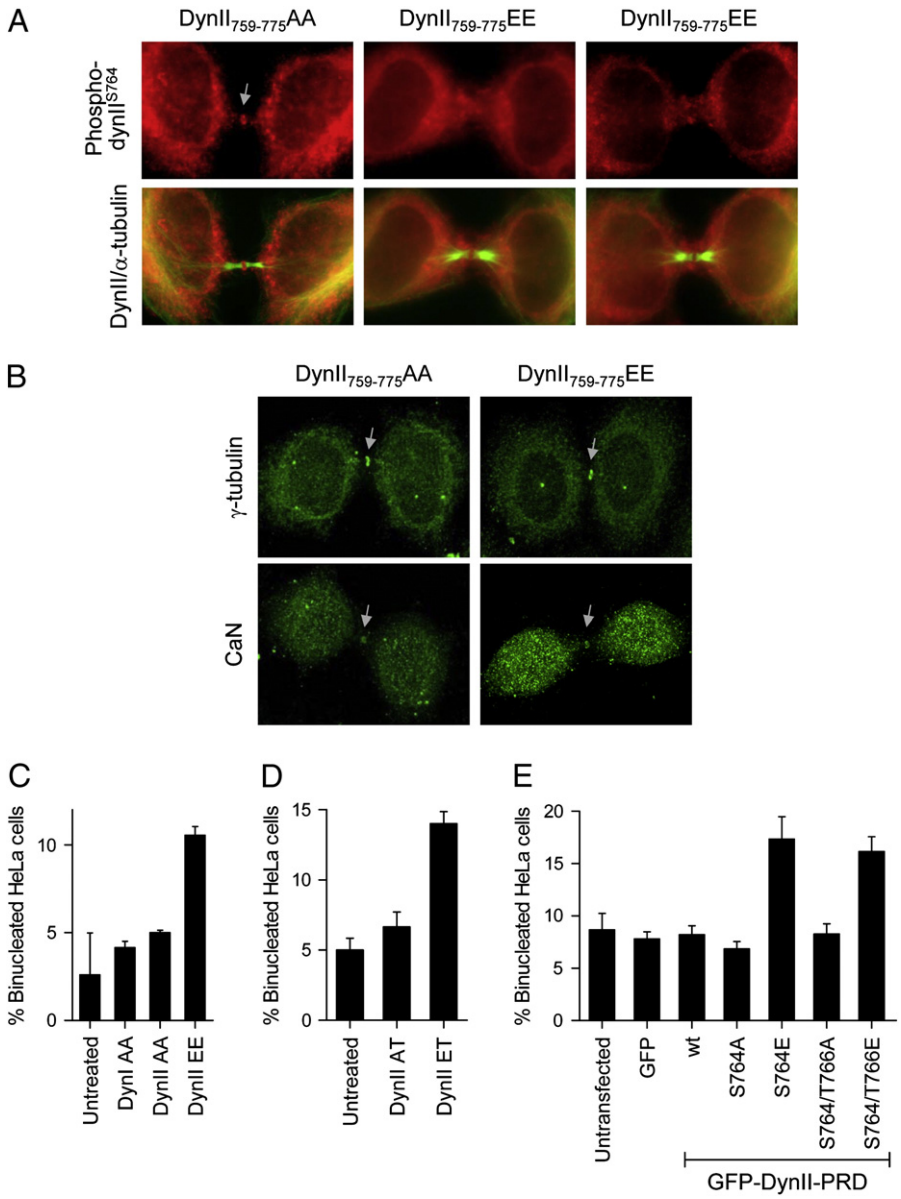

Fig. 6. Phospho-dynII localises to the midbody. (A and B) Representative immunofluorescence microscopy images of HeLa cells treated with the phospho-deficient or phospho-mimetic dynII peptides, then stained for phospho-dynII (A) and γ-tubulin (B, upper panels) and CaN (B, lower panels). Phospho-dynII staining is enriched at the midbody (not shown; [18]) and this was not affected by the phospho-deficient peptide, dynII$_{759-775}$AA (left). However, the phospho-mimetic peptide, dynII$_{759-775}$EE, prevents phospho-dynII recruitment to the midbody (red; two examples are shown on the right) without affecting the localisation of the midbody components, γ-tubulin and CaN. (C) The dynII$_{759-775}$EE phospho-mimetic peptide causes cytokinesis failure. HeLa cells were synchronised at the G_1/S transition by double thymidine block. At 8 h post-release from the block, cells were incubated in the presence or absence of either penetratin phospho-box peptide (100 μM). Cells were subsequently stained for α-tubulin and phospho-dynII. The graph displays the mean ± SD from at least two independent experiments. (D) HeLa cells were synchronised at the G_2/M transition using RO-3306. Immediately following release from this block, cells were incubated for 6 h in the presence or absence of a penetratin phospho-box peptide (100 μM) whereby only the Ser-764 is mutated (dynII$_{759-775}$AT and dynII$_{759-775}$ET). Cells were subsequently stained for α-tubulin. The graph displays the mean ± SD from two independent experiments. (E) HeLa cells ectopically expressing wild-type, phospho-mimetic (S764E and S764/T766E) and phospho-deficient (S764A and S764/T766A) mutants of GFP–dynII–PRD were fixed 72 h post-transfection, stained for α-tubulin and scored for multinucleation. The graph displays the mean ± SD from at least two independent experiments.

of cells treated with the phospho-mimetic peptide dynII$_{759-775}$EE (Fig. 6A, upper panels). CaN and γ-tubulin midbody localisation was unaffected (Fig. 6B, lower panels). This suggests that phospho-dynII localization to the midbody is dependent in its phosphorylation status, while CaN localization to the midbody is not dependent on dynII. Again, full length GFP–dynII did not target the midbody when ectopically expressed in HeLa cells and therefore could not be used to address this question. The results suggest a role for Ser-764 phosphorylation in regulating dynII localisation during cytokinesis.

To test whether dynII phosphorylation is involved in cytokinesis, we examined multinucleation, which is a characteristic of failed cytokinesis. The phospho-mimetic dynII$_{759-775}$EE peptide significantly increased multinucleation, indicating cytokinesis failure due to displacement of dynII rather than CaN (Fig. 6C). The phospho-deficient peptides from either dynII or dynI were without effect, suggesting that the observation is specific. We initially chose the EE mutant to increase the net negative charge in this region since phosphorylation carries two negative charges while E mutants carry only one. Similar results were obtained with an identical dynII peptide wherein only the Ser-764 was mutated (Fig. 6D, peptides are named AT or ET to indicate that the Thr-766 is wild-type). This is consistent with the major role being ascribed only to the Ser-764 phosphosite.

We next aimed to confirm the link between dynII phosphorylation at Ser-764 and cytokinesis by an independent approach. Again, full length GFP–dynII did not target the midbody when ectopically expressed in HeLa cells. Therefore, it could not be used to address the question. However, analogous to endogenous dynII, the dynII–PRD region (GFP–dynII–PRD) when ectopically expressed, localised to the midbody. Overexpression of this form of dynII containing phospho-mimetic mutations (S764E or S764E/T766E) caused a specific increase in multinucleation compared to the equivalent phospho-deficient (S764A or S764A/T766A) and wild-type forms (Fig. 6E). This confirms that Ser-764, not Thr-766, is the phosphosite that is associated with cytokinesis in a cellular context. The results suggest that dynII phosphorylation is important for cytokinesis.

4. Discussion

CaN triggers events late in mitosis that appear to trigger cellular abscission at the end of cytokinesis [18]. This involves dephosphorylation of dynII and potentially many other CaN substrates at the midbody. DynII has recently been shown to be mitotically phosphorylated on Ser-764 and/or Thr-766 [19]. We have now significantly extended these observations by showing that dynII is phosphorylated exclusively at Ser-764 specifically during mitosis and that this phosphosite appears to be involved in cytokinesis rather than endocytosis or centrosome cohesion. Thus, phosphorylation switches the function of dynII from a traditional to a novel role. Our findings strongly suggest that not just CaN but CaN-mediated dynII dephosphorylation is an essential molecular component of cytokinesis, as CaN alone at the midbody is insufficient to complete cytokinesis in the absence of dynII. To our surprise, dynII phosphorylation did not affect other known biological roles for dynII such as CME or bulk endocytosis, suggesting that phosphorylation is specific to its cytokinesis role. This is surprisingly analogous to dynI, the phosphorylation of which switches the function of dynI from clathrin-dependent synaptic vesicle endocytosis to activity-dependent bulk endocytosis in neurons [6,11,12]. Our findings suggest that phosphorylation of dynamin directs it to a new role in cytokinesis that is independent of its well-characterised role in classical endocytosis.

This is the first report of directly validated dynII phosphorylation on serine or threonine residues. Mass spectrometry analysis suggests that there is only a single phosphosite in dynII at the onset of mitosis, although non-detectable minor sites may exist, strongly contrasting to multi-site phosphorylation of dynI and III in neurons [9]. Phosphorylation at Ser-764 was independently confirmed by three approaches: MS analysis on dynII in rat lung, HeLa cells and using phosphosite-specific antibodies. Neither dynI protein nor phosphorylation of its abundant site at Ser-774 was detected with any approach. No dynII phosphorylation on tyrosine was detected in our study, but this cannot be ruled out due to its lability. In contrast, other studies suggest a role for tyrosine phosphorylation at the Golgi during vesicle trafficking [17], which is normally stopped during mitosis but resumes during cytokinesis [36–38]. Given that dynI is phosphorylated on 7 sites and dynIII on 3 sites in synaptosomes [9], it is perhaps surprising that we found only 1 phosphosite in dynII in rat lung or HeLa cells within methodological detection limits, despite our extensive efforts to search for more. Mono-phosphorylation of a protein in cells is far less common than multi-site phosphorylation. However, among the phosphosites identified in the other classical dynamins, only two (Ser-347/778) are conserved in the sequence of dynII (as dynII-347 and Ser-764). Ser-347 does not have the amino acid consensus motif required for mitotic phosphorylation, resides in an acidic amino acid environment (IEGSGDQVD) and is the lowest abundance site in dynI. Therefore, it is not surprising that its phosphorylation in rat lungs or HeLa cells was undetectable.

Two large-scale phosphoproteomic studies reported that dynII from mitotic cells is phosphorylated on a single tryptic phosphopeptide ($dynII_{731–769}$), in agreement with our work [22,23]. However, these studies listed all four phosphorylatable sites (S/T/Y) between Ser-761 and Thr-766 as phosphorylated in HeLa cells (the tryptic peptide is EALNIIGDISTSTVSTPVPPPVDDTWLQSASSH**pS**PTPQR$_{731–769}$, sites are underlined; Ser-764 is in bold). All four phosphosite results were subsequently transferred to a public phosphosite database (www.phosphosite.org). We believe that these sites in dynII were prematurely given the status of genuine phosphorylation sites. Ser-764 is the only genuine phosphosite and evidence supports this conclusion (see Supplementary information for a detailed discussion).

Our phosphosite assignment has been validated by detection of phospho-dynII–Ser-764 using phospho-specific antibodies to this site both after *in vitro* phosphorylation and in cells. Additionally, the recombinant form of dynII where this site was mutated to Ala lost over 80% of its *in vitro* phosphorylation by cdk, indicating that Ser-764 is the main phosphosite *in vitro* as well as in cells. Finally, endogenous dynII did not localise to the midbody in cells treated with the dynII phospho-mimetic peptide whereby only the Ser-764 was mutated to Glu and the Thr-766 was wild-type (data not shown), indicating that the functional role is only for Ser-764 in cells. Note that *in vitro* phosphosites are only indicative of phosphosites that might be found in cells but cannot be used as evidence for the presence or not of that site in cells.

The mitotic phosphorylation site in dynII clearly did not play an essential role in CME or bulk endocytosis as determined by two independent strategies of peptide competition and siRNA depletion/rescue. For example, we found that both phospho-deficient and phospho-mimetic GFP–dynII constructs could completely rescue CME. This is consistent with the known ability of such wild-type constructs to rescue endocytosis [1] and suggests that Ser-764 is not required. This observation is consistent with recent studies on mitotic endocytosis. At least three other endocytic proteins are phosphorylated upon mitotic entry: epsin, eps15 and amphiphysin I. While their phosphorylation in nerve terminals appears to be related to inhibiting their role in endocytosis until they are dephosphorylated by calcineurin, they were originally proposed to be mitotically phosphorylated in order to inhibit endocytosis during mitosis. However, a recent study suggests that endocytosis is not specifically inhibited in mitotic cells [39]. This suggests that mitotic phosphorylation of key endocytic proteins may be a common mitotic event with a role in functions other than endocytosis. In support of this idea, epsin induces membrane curvature for proper mitotic spindle organisation and this role is independent of its endocytic function and mitotic phosphorylation [40]. In an analogous manner to dynII–Ser-764, it is also possible that these other mitotically phosphorylated endocytic proteins might prove to be CaN targets during cytokinesis.

Phosphorylation of dynII at Ser-764 in the phospho-box region by cdk1 coincided with its localisation to the centrosome where it resided until late in mitosis. It is unclear whether there is any role for phosphorylation here since we observed no specific centrosome defects in dynII-depleted cells (data not shown). Like dynII, many other proteins are phosphorylated upon mitotic entry and locate to the mitotic centrosome [41]. This localisation is thought to be driven by phosphorylation. However, our data suggest that Ser-764 phosphorylation is not required for targeting dynII to the mitotic centrosome. This is consistent with previous findings demonstrating that the dynamin middle domain binds the centrosome component, γ-tubulin [3]. We confirmed that the middle domain of dynII, when fused to GFP, targets the centrosome, while the full length protein did not. This suggests that full length dynII constructs (GFP or Flag-tagged) do not fully mimic all of the biological roles of endogenous dynII. Many cytokinesis proteins, such as Cep55, reside at the centrosome during mitosis without any known centrosome role [41,42]. The role of phospho-dynII on the mitotic centrosome is unclear; however, one possibility is that it is an intermediate "holding" location for certain proteins that are involved in later mitotic events. In contrast to phospho-dynII, CaN does not locate to

the mitotic centrosome [18]. Therefore, the centrosome location of phospho-dynII may provide a mechanism of physically separating it from CaN at this point in mitosis. For example, Ca^{2+} activates CaN and acts at a second point in mitosis, prior to cytokinesis during anaphase progression [43,44]. The lack of CaN/dynII colocalisation at this stage may conceivably protect dynII from being prematurely dephosphorylated and hence triggering mitotic exit prematurely.

Collectively, our observations highlight a molecular signalling pathway that is associated with completion of the abscission stage of cytokinesis that involves Ca^{2+}, CaN and phospho-dynII–Ser-764. This is strikingly analogous to dynI where an analogous signalling pathway and phosphosites regulate the switching of the standard synaptic vesicle endocytic mode to a second unique bulk endocytosis role [6,11,12]. Our two recent discoveries demonstrate that CaN activity [18] and dynII [1,2,4,34,35] are required for the completion of the abscission stage of cytokinesis. Here, we now show that it is the phosphorylated form of dynII that is a key part of the cytokinesis mechanisms downstream of CaN rather than playing a role in endocytosis. We found phospho-dynII is concentrated at the midbody at the time of cytokinesis [18]. In contrast to the centrosome, this localisation was disrupted by the phospho-mimetic peptides but not by phospho-deficient peptides. It is possible that Ser-764 phosphorylation is a signal to target or tether dynII to the midbody during cytokinesis with its dephosphorylation releasing it into partnership with a specific, as yet unidentified, phospho-dependent binding partner. The phospho-mimetic peptides specifically induced cytokinesis failure, as indicated by a significant increase in multinucleation, a primary characteristic of failed cytokinesis. The dynII phospho-mimetic peptides had no effect on CaN midbody localisation; thus, CaN alone at the midbody is not sufficient to complete cytokinesis. Instead, these findings collectively suggest that CaN-mediated dephosphorylation of dynII–Ser-764 is associated with successful completion of cytokinesis. We also found that a GFP–dynII–PRD construct targeted the midbody and that cells expressing GFP–dynII–PRD phospho-mimetic mutants, not phospho-deficient mutants, increased cytokinesis failure. Overall, our data show that dynII is mitotically phosphorylated primarily on a single site, Ser-764 by cdk, and that this phosphorylation site is not involved in endocytosis or centrosome cohesion but rather in the regulation of cytokinesis.

Acknowledgements

We wish to thank Sandra L Schmid and Jenny Stow for providing the baculovirus purified dynII protein and GFP-α-tubulin, respectively. Anna Powell is thanked for her technical assistance. This work was supported by grants from the National Health and Medical Research Council (NH&MRC) of Australia (PJR), the NH&MRC Peter Doherty and Biomedical Career Development Fellowships (MC), the Ramaciotti Foundation, the Australian Cancer Research Foundation, Cancer Institute NSW and Ian Potter Foundation.

All authors declare no conflict of interest.

Appendix A. Supplementary data

Supplementary data to this article can be found online at doi:10.1016/j.bbamcr.2010.12.018.

References

[1] Y.W. Liu, M.C. Surka, T. Schroeter, V. Lukiyanchuk, S.L. Schmid, Isoform and splice-variant specific functions of dynamin-2 revealed by analysis of conditional knock-out cells, Mol. Biol. Cell 19 (2008) 5347–5359.
[2] H.M. Thompson, A.R. Skop, U. Euteneuer, B.J. Meyer, M.A. McNiven, The large GTPase dynamin associates with the spindle midzone and is required for cytokinesis, Curr. Biol. 12 (2002) 2111–2117.
[3] H.M. Thompson, H. Cao, J. Chen, U. Euteneuer, M.A. McNiven, Dynamin 2 binds gamma-tubulin and participates in centrosome cohesion, Nat. Cell Biol. 6 (2004) 335–342.
[4] S. Joshi, S. Perera, J. Gilbert, C.M. Smith, C.P. Gordon, A. McCluskey, J.A. Sakoff, A. Braithwaite, P.J. Robinson, M. Chircop (nee Fabbro), The dynamin inhibitors MiTMAB and OcTMAB induce cytokinesis failure and inhibit cell proliferation in human cancer cells, Mol. Cancer Ther. 9 (2010) 1995–2006.
[5] G.J.K. Praefcke, H.T. McMahon, The dynamin superfamily: universal membrane tubulation and fission molecules? Nat. Rev. Mol. Cell Biol. 5 (2004) 133–147.
[6] M.A. Cousin, P.J. Robinson, The dephosphins: dephosphorylation by calcineurin triggers synaptic vesicle endocytosis, Trends Neurosci. 24 (2001) 659–665.
[7] S. Sever, A.B. Muhlberg, S.L. Schmid, Impairment of dynamin's GAP domain stimulates receptor-mediated endocytosis, Nature 398 (1999) 481–486.
[8] T.C. Tan, V.A. Valova, C.S. Malladi, M.E. Graham, L.A. Berven, O.J. Jupp, G. Hansra, S.J. McClure, B. Sarcevic, R.A. Boadle, M.R. Larsen, M.A. Cousin, P.J. Robinson, Cdk5 is essential for synaptic vesicle endocytosis, Nat. Cell Biol. 5 (2003) 701–710.
[9] M.E. Graham, V. Anggono, N. Bache, M.R. Larsen, G.E. Craft, P.J. Robinson, The in vivo phosphorylation sites of rat brain dynamin I, J. Biol. Chem. 282 (2007) 14695–14707.
[10] Y. Huang, M.C. Chen-Hwang, G. Dolios, N. Murakami, J.C. Padovan, R. Wang, Y.W. Hwang, Mnb/Dyrk1A phosphorylation regulates the interaction of dynamin 1 with SH3 domain-containing proteins, Biochemistry 43 (2004) 10173–10185.
[11] J.P. Liu, A.T.R. Sim, P.J. Robinson, Calcineurin inhibition of dynamin-I GTPase activity coupled to nerve-terminal depolarization, Science 265 (1994) 970–973.
[12] E.L. Clayton, V. Anggono, K.J. Smillie, N. Chau, P.J. Robinson, M.A. Cousin, The phospho-dependent dynamin–syndapin interaction triggers activity-dependent bulk endocytosis of synaptic vesicles, J. Neurosci. 29 (2009) 7706–7717.
[13] V. Anggono, K.J. Smillie, M.E. Graham, V.A. Valova, M.A. Cousin, P.J. Robinson, Syndapin I is the phosphorylation-regulated dynamin I partner in synaptic vesicle endocytosis, Nat. Neurosci. 9 (2006) 752–760.
[14] V. Anggono, P.J. Robinson, Syndapin I and endophilin I bind overlapping proline-rich regions of dynamin I: role in synaptic vesicle endocytosis, J. Neurochem. 102 (2007) 931–943.
[15] S. Ahn, J. Kim, C.L. Lucaveche, M.C. Reedy, L.M. Luttrell, R.J. Lefkowitz, Y. Daaka, Src-dependent tyrosine phosphorylation regulates dynamin self-assembly and ligand-induced endocytosis of the epidermal growth factor receptor, J. Biol. Chem. 277 (2002) 26642–26651.
[16] A.N. Shajahan, B.K. Timblin, R. Sandoval, C. Tiruppathi, A.B. Malik, R.D. Minshall, Role of Src-induced dynamin-2 phosphorylation in caveolae-mediated endocytosis in endothelial cells, J. Biol. Chem. 279 (2004) 20392–20400.
[17] S.G. Weller, M. Capitani, H. Cao, M. Micaroni, A. Luini, M. Sallese, M.A. McNiven, Src kinase regulates the integrity and function of the Golgi apparatus via activation of dynamin 2, Proc. Natl Acad. Sci. USA (2010).
[18] M. Chircop, C.S. Malladi, A.T. Lian, S.L. Page, M. Zavortink, C.P. Gordon, A. McCluskey, P.J. Robinson, Calcineurin activity is required for the completion of cytokinesis, Cell. Mol. Life Sci. 67 (2010) 3725–3737.
[19] M. Morita, K. Hamao, S. Izumi, E. Okumura, K. Tanaka, T. Kishimoto, H. Hosoya, Proline-rich domain in dynamin-2 has a low microtubule-binding activity: how is this activity controlled during mitosis in HeLa cells? J. Biochem. 148 (2010) 533–538.
[20] H. Chen, V.I. Slepnev, P.P. Di Fiore, P. De Camilli, The interaction of epsin and Eps15 with the clathrin adaptor AP-2 is inhibited by mitotic phosphorylation and enhanced by stimulation-dependent dephosphorylation in nerve terminals, J. Biol. Chem. 274 (1999) 3257–3260.
[21] S.R. Floyd, E.B. Porro, V.I. Slepnev, G.C. Ochoa, L.H. Tsai, P. De Camilli, Amphiphysin 1 binds the cyclin-dependent kinase (cdk) 5 regulatory subunit p35 and is phosphorylated by cdk5 and cdc2, J. Biol. Chem. 276 (2001) 8104–8110.
[22] S.A. Beausoleil, M. Jedrychowski, D. Schwartz, J.E. Elias, J. Villen, J. Li, M.A. Cohn, L.C. Cantley, S.P. Gygi, Large-scale characterization of HeLa cell nuclear phosphoproteins, Proc. Natl Acad. Sci. USA 101 (2004) 12130–12135.
[23] N. Dephoure, C. Zhou, J. Villen, S.A. Beausoleil, C.E. Bakalarski, S.J. Elledge, S.P. Gygi, A quantitative atlas of mitotic phosphorylation, Proc. Natl Acad. Sci. USA 105 (2008) 10762–10767.
[24] A. Quan, P.J. Robinson, Rapid purification of native dynamin I and colorimetric GTPase assay, Meth. Enzymol. 404 (2005) 556–569.
[25] M. Chircop, V. Oakes, M.E. Graham, M.P. Ma, C.M. Smith, P.J. Robinson, K.K. Khanna, The actin-binding and bundling protein, EPLIN, is required for cytokinesis, Cell Cycle 8 (2009) 757–764.
[26] L.T. Vassilev, C. Tovar, S.Q. Chen, D. Knezevic, X.L. Zhao, H.M. Sun, D.C. Heimbrook, L. Chen, Selective small-molecule inhibitor reveals critical mitotic functions of human CDK1, Proc. Natl Acad. Sci. USA 103 (2006) 10660–10665.
[27] B. Sarcevic, R. Lilischkis, R.L. Sutherland, Differential phosphorylation of T-47D human breast cancer cell substrates by D1-, D3-, E-, and A-type cyclin–CDK complexes, J. Biol. Chem. 272 (1997) 33327–33337.
[28] M.R. Larsen, T.E. Thingholm, O.N. Jensen, P. Roepstorff, T.J.D. Jorgensen, Highly selective enrichment of phosphorylated peptides from peptide mixtures using titanium dioxide microcolumns, Mol. Cell Prot. 4 (2005) 873–886.
[29] G.E. Craft, M.E. Graham, N. Bache, M.R. Larsen, P.J. Robinson, The in vivo phosphorylation sites in multiple isoforms of amphiphysin I from rat brain nerve terminals, Mol. Cell. Proteomics 7 (2008) 1146–1161.
[30] T.A. Hill, C.P. Gordon, A.B. McGeachie, B. Venn-Brown, L.R. Odell, N. Chau, A. Quan, A. Mariana, J.A. Sakoff, M. Chircop, P.J. Robinson, A. McCluskey, Inhibition of dynamin mediated endocytosis by the dynoles—synthesis and functional activity of a family of indoles, J. Med. Chem. 52 (2009) 3762–3773.
[31] L.R. Odell, D. Howan, C.P. Gordon, M.J. Robertson, N. Chau, A. Mariana, A.E. Whiting, R. Abagyan, J.A. Daniel, N.N. Gorgani, P.J. Robinson, A. McCluskey, The

pthaladyns: GTP competitive inhibitors of dynamin I and II GTPase derived from virtual screening, J. Med. Chem. 53 (2010) 5267–5280.
[32] N. Taguchi, N. Ishihara, A. Jofuku, T. Oka, K. Mihara, Mitotic phosphorylation of dynamin-related GTPase Drp1 participates in mitochondrial fission, J. Biol. Chem. 282 (2007) 11521–11529.
[33] M.A. Cousin, Synaptic vesicle endocytosis—calcium works overtime in the nerve terminal, Mol. Neurobiol. 22 (2000) 115–128.
[34] B. Feng, H. Schwarz, S. Jesuthasan, Furrow-specific endocytosis during cytokinesis of zebrafish blastomeres, Exp. Cell Res. 279 (2002) 14–20.
[35] H.M. Thompson, A.R. Skop, M.A. McNiven, Dynamin is a component of the intercellular bridge and is required for cytokinesis in hepatocytes, Hepatol. 36 (2002) 212A.
[36] R. Albertson, B. Riggs, W. Sullivan, Membrane traffic: a driving force in cytokinesis, Trends Cell Biol. 15 (2005) 92–101.
[37] G.M. Gaietta, B.N. Giepmans, T.J. Deerinck, W.B. Smith, L. Ngan, J. Llopis, S.R. Adams, R.Y. Tsien, M.H. Ellisman, Golgi twins in late mitosis revealed by genetically encoded tags for live cell imaging and correlated electron microscopy, Proc. Natl Acad. Sci. USA 103 (2006) 17777–17782.
[38] J.W. Goss, D.K. Toomre, Both daughter cells traffic and exocytose membrane at the cleavage furrow during mammalian cytokinesis, J. Cell Biol. 181 (2008) 1047–1054.
[39] E. Boucrot, T. Kirchhausen, Endosomal recycling controls plasma membrane area during mitosis, Proc. Natl. Acad. Sci. U.S. A. 104 (2007) 7939–7944.
[40] Z. Liu, Y. Zheng, A requirement for epsin in mitotic membrane and spindle organization, J. Cell Biol. 186 (2009) 473–480.
[41] S. Doxsey, D. McCollum, W. Theurkauf, Centrosomes in cellular regulation, Annu. Rev. Cell Dev. Biol. 21 (2005) 411–434.
[42] M. Fabbro, B.B. Zhou, M. Takahashi, B. Sarcevic, P. Lal, M.E. Graham, B.G. Gabrielli, P.J. Robinson, E.A. Nigg, Y. Ono, K.K. Khanna, Cdk1/Erk2- and Plk1-dependent phosphorylation of a centrosome protein, Cep55, is required for its recruitment to midbody and cytokinesis, Dev. Cell 9 (2005) 477–488.
[43] L. Groigno, M. Whitaker, An anaphase calcium signal controls chromosome disjunction in early sea urchin embryos, Cell 92 (1998) 193–204.
[44] R. Wong, I. Hadjiyanni, H.C. Wei, G. Polevoy, R. McBride, K.P. Sem, J.A. Brill, PIP2 hydrolysis and calcium release are required for cytokinesis in Drosophila spermatocytes, Curr. Biol. 15 (2005) 1401–1406.